Conditions of Elaboration of Luminescent Porous Silicon from Hydrogenated Amorphous Silicon

R. B. Wehrspohn, J.-N. Chazalviel, F. Ozanam, and I. Solomon
Centre National de la Recherche Scientifique, École Polytechnique, Laboratoire de Physique de la Matière Condensée, 91128 Palaiseau Cedex, France
(Received 7 February 1996)

We present a systematic study of the preparation and properties of porous silicon obtained by anodic etching of device-grade hydrogenated amorphous silicon. Highly luminescent porous material is produced from boron-doped films and, by hole injection, from undoped films. A striking difference between amorphous and crystalline Si lies in an electrochemical instability which limits the maximum obtainable thickness in porous material. The luminescence mechanism for porous *a*-Si:H appears to be markedly different from that of its crystalline counterpart. [S0031-9007(96)01068-X]

PACS numbers: 78.55.Mb, 73.61.Jc, 78.66.Jg, 82.45.+z

The efficient photoluminescence (PL) of porous silicon at room temperature has inspired an unprecedented worldwide research effort [1]. Most of the published studies concern the material obtained by anodization of crystalline silicon (*c*-Si) wafers in a hydrofluoric acid electrolyte. Preliminary attempts to prepare luminescent porous material from hydrogenated amorphous silicon, *a*-Si:H, gave negative results [2]. A successful result was reported by Bustarret *et al.* [3–5] with heavily boron-doped *a*-Si:H. We present here a systematic study of the preparation and properties of porous silicon obtained by anodic etching of device-grade hydrogenated amorphous silicon, the material optimized for the fabrication of high-efficiency photocells. Thin films of photoluminescent porous silicon have been obtained with undoped material as well as with *p*-type materials, with a boron doping ranging from 0.05% to 1.5%. The preparation with undoped films was performed with a special technique of hole injection from a heavily doped p^+ electrode. The formation of porous silicon [6] and the microscopic processes involved in the spectacular luminescence of this material are still a subject of controversy [1]. It is therefore of importance to compare with porous silicon prepared from a different precursor.

The *a*-Si:H films are produced by rf-plasma decomposition of pure silane SiH_4 in a capacitively coupled reactor at 13.56 MHz. Normal deposition conditions are total pressure, 50 mTorr; gas flow rate, 2 l/h; rf power density, 0.15 W/cm^2; substrate temperature, 250 °C. These values are known to produce a homogeneous, low density-of-state amorphous material, far from the conditions of production of microcrystalline material [7]. The amorphous deposited material is of device grade, with a gap defined by $E_{04} = 190$ eV and a density of states at the Fermi level (determined by space-charge limited current measurements) of about 4×10^{15} cm^{-3} eV^{-1} for the undoped material. Boron doping is obtained by injecting a small amount of a mixture of diborane gas and hydrogen (3% of B_2H_6 in H_2) into the plasma. The films are deposited on optically polished stainless steel. The resistivity of the boron-doped samples varies from 10^4 to 10^6 Ω cm when the diborane content varies from 6% to 0.05%.

The electrochemical cell is made of polytrifluorochloroethylene, with a Ag/AgCl reference and platinum counterelectrode. For *a*-Si:H there are no published data concerning the anodizing conditions. We had therefore to perform a lengthy and tedious exploration of the "space of preparation," varying HF concentration (5% to 50%) and current density (1 to 30 mA/cm^2). Finally, we found that 25% of HF (HF/H_2O/ethanol in the ratio 5/9/6) and 10 mA/cm^2 makes a reproducible and reasonably good luminescent material at all doping levels, and these conditions were taken as a standard for the present study. The voltammetric curves in diluted HF are essentially the same for *c*-Si and *a*-Si:H, which suggests that the basic electrochemistry is the same for both materials. Infrared spectroscopy shows that the porous materials are identically coated with Si-H bonds and exhibit comparable surface areas. This leads us to conclude that the size of the nanostructures is of the same order of magnitude in both materials. No Si-O bonds have been detected by Fourier transform infrared spectroscopy. In contrast with crystalline porous silicon [1], the porous material thus obtained is stable in time (see below), and no postoxidation has been carried out for our samples.

A major difference between *a*-Si:H and *c*-Si is shown in Fig. 1: We plot a typical variation of the film potential (compared to the reference electrode) as a function of time during the galvanostatic anodization of a film of boron-doped *a*-Si:H (we note that for a wafer of crystalline silicon, this potential would be constant). We observe three different regimes during the anodization: a "uniform mode," in which the potential decreases linearly in time (region A); then an "unstable mode," with the onset of a strongly nonlinear and noisy decrease of the potential (region B); and finally (region C), the potential reaches a nearly constant value of 0.4 V, corresponding to the anodization potential of the heavily doped contact layer on the substrate. Eventually the amorphous layer peels

0031-9007/96/77(9)/1885(4)$10.00 © 1996 The American Physical Society

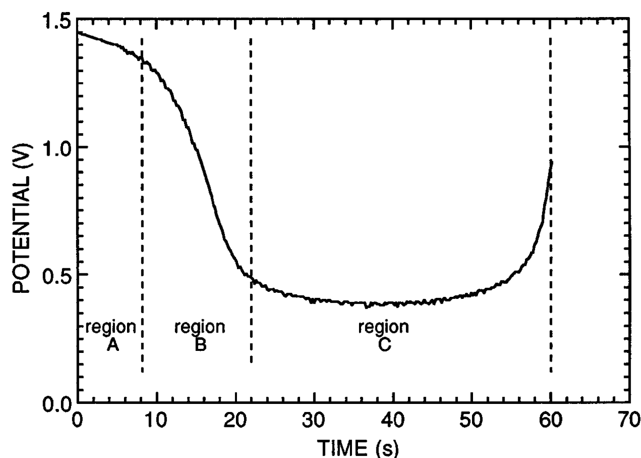

FIG. 1. Variation of the electrode potential ($E_{\mathrm{electrode}} - E_{\mathrm{reference}}$) as a function of the etching time for a current density of 10 mA/cm^2. We observe three regions as discussed in the text. Region A ("uniform mode") corresponds to the formation of porous silicon. The following two regions B and C correspond to instabilities that do not exist for *c*-Si. The sample is a 0.38% boron-doped layer (2 μm) of *a*-Si:H on stainless steel.

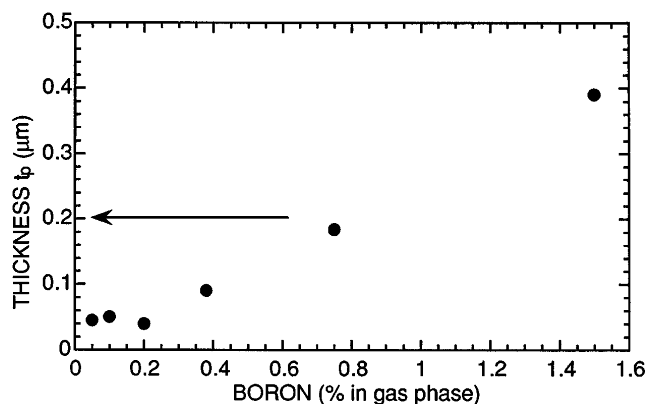

FIG. 2. Thickness t_p of the porous layer obtained during the uniform mode (region A in Fig. 1) before the onset of instabilities of regions B and C. The arrow shows the thickness of a thin undoped film wholly made porous, the holes for anodization being produced by injection from a heavily doped electrode (see text).

off, and the potential rises to the value corresponding to the anodization of the stainless steel substrate.

We relate the uniform mode of the first region to the same pore formation process as in crystalline silicon. The slight decrease of the potential is due to the decrease of the thickness of the unaffected part of the amorphous layer during anodization. The thickness t_p of the porous layer produced during this mode has been determined by reflection interferometry. We observe that it is strongly dependent on the doping level, as shown in Fig. 2. The strong variation of the potential in region B is a new phenomenon, which does not appear in anodization of *c*-Si. Surprisingly, we observe no significant increase of the porous layer thickness during this mode although the potential varies rapidly. We are then led to assume that the current flows through filaments across the *a*-Si film. The fast decrease of the potential corresponds to a progressive short-circuiting of the *a*-Si layer by the growing channels. These channels can indeed be observed by AFM and SEM [8]. They tend to be perpendicular to the film, with a diameter of about 200 to 400 nm and a density of a few per μm^2. When we continue the anodization, the filaments keep growing until they reach the heavily doped contact layer of 1000 Å deposited on the stainless steel substrate to provide the Ohmic contact. This layer is progressively etched out at a constant potential (region C) due to the negligible value of the Ohmic drop, until eventually there is a fast peeling off of the silicon film.

The onset of an unstable mode which stops the pore formation after a while is a new effect, specific to the anodization of *a*-Si films. In practice, this severely limits the thickness of porous films that can be obtained with *a*-Si:H (Fig. 2). We relate this effect to the relatively high value of the resistivity of the amorphous material. Based on very simple electrostatic considerations we have been able to model quantitatively the evolution of the electrolyte/*a*-Si:H interface. The important parameter is the ratio of the resistivity of the silicon material to that of the electrolyte. The situation is very different for crystalline and amorphous silicon: The resistivity of *c*-Si used for anodization (0.1 to 10 Ω cm) is smaller than or similar to that of the electrolyte, whereas the resistivity of *a*-Si:H is some 10^4 to 10^6 times larger, depending on the doping level. This explains the differences in anodization properties between the two materials. The detailed calculation is to be published elsewhere [8], but the qualitative physical principles are quite simple. For *c*-Si, the potential drop, during anodization, occurs mostly at the semiconductor/electrolyte interface, there is no electrostatic evolution during the silicon etching and the pore formation continues regularly. For *a*-Si:H, because of its high resistivity, the situation is reversed: The electrolyte is more conducting than the silicon. Therefore, a fluctuation-induced filament will carry more current than the surrounding solid. The length of the filament will then increase by etching of the silicon, and the filament will eventually pierce the whole layer. The more resistive the material, the more pronounced the effect is, as can be seen in Fig. 2: For low-doped material the porous-layer formation stops after 500 Å, whereas for a 1.5%-doped sample, a thickness of 0.4 μm can be obtained. It probably explains why the porous material from *a*-Si:H was first observed with heavily doped *a*-Si:H [3]. Finally, since this instability originates from the differences of resistivities between the solid and the electrolyte, we can predict that the thickness t_p of the porous material can be increased

by using a more resistive electrolyte. Some preliminary experiments have shown that it is indeed the case.

Because anodic dissolution requires the presence of holes for normal pore formation [6], *p*-type material is generally used. For near intrinsic or *n*-type silicon, pore formation can be obtained only under illumination, by photoinjection of carriers. A novel and more elegant method of providing the necessary holes has been used for our undoped films of *a*-Si:H. We use *electrical injection,* based on the fact that a p^+-i structure, necessary for an Ohmic contact with the substrate, is also a perfectly injecting electrode. But the density of injected carriers is severely limited by the induced space charge (space-charge limited current, see, for example, [9]). The space-charge potential increases rapidly with the thickness L of the sample (like L^2 [10]). Amorphous silicon samples, with a thin film geometry in the μm range, allow high levels of injection that would be difficult to obtain with a crystalline silicon wafer many times thicker [11]. This method has been applied to a very thin film of 0.2 μm in a p^+-i configuration [(stainless steel)/(0.1 μm of 2% boron doped)/(0.2 μm of undoped *a*-Si:H)]. For a current density of 10 mA/cm^2, the density of injected holes is equivalent to the density that can be obtained with a boron doping of about 1%. Thus the whole undoped layer has been made porous, as indicated by the arrow in Fig. 2. This method has several advantages over light illumination. It allows the injection of *one type of carrier* only (holes in the present case). Electrical injection is easier to control quantitatively than photoinjection. And also, the porous material is produced from low density-of-states, boron-free material, which is more favorable for a good luminescence efficiency.

The porous silicon samples are excited by the 476 nm line of a Kr^+ laser. The laser beam is directed unfocused on the sample which is kept in air for room-temperature measurements or in a transparent electrochemical cell for *in situ* PL [12]. The power density is 10 mW/cm^2. Boron-doped material has a high density of states in the gap and shows no luminescence even at low temperature. After electrochemical treatment, amorphous layers exhibit room-temperature PL with a peak energy of 1.3 to 1.5 eV depending on the anodization conditions and doping level (Fig. 3). The absolute PL intensity of porous *a*-Si:H is rather weak, which makes it hardly visible to the naked eye. This is not due to a low quantum efficiency, but to the small thickness obtained by anodization of the *a*-Si:H layer. When comparing samples with the same electrochemical treatment and similar thickness, the PL intensities of porous *a*-Si:H and porous crystalline material are of the same order of magnitude (Fig. 3). However, under conditions leading to optimum PL of porous *c*-Si, the PL intensity of porous *a*-Si:H is generally smaller. The luminescence observed under an optical microscope of about 1 μm resolution is homogeneous, contrary to what has been observed by Bustarret *et al.* [4] for heavily doped silicon. It is to be expected that larger-gap materials would show a PL peak at higher energy. Preliminary experiments have shown that the luminescence peak energy for an amorphous silicon-carbon alloy (with 10% carbon) is indeed shifted to a value of 1.72 eV. Under intense UV irradiation (351 nm, ~150 mW/cm^2), the photodegradation of porous *a*-Si:H in air at room temperature is clearly smaller than that of porous *c*-Si (Fig. 4).

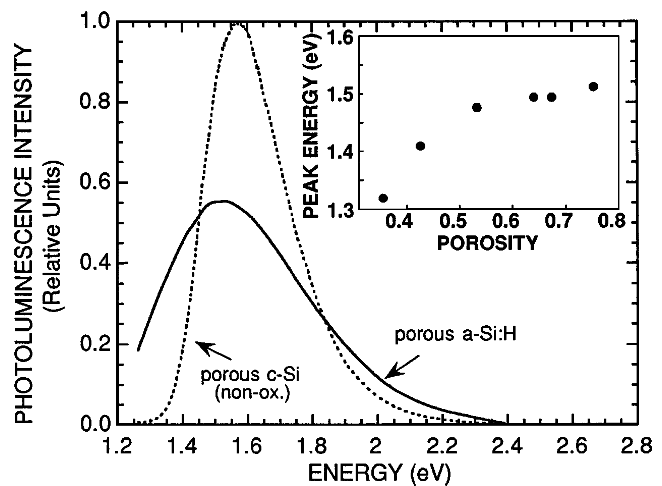

FIG. 3. Comparison of the photoluminescence spectra of porous silicon obtained from *a*-Si:H with that of nonoxidized crystalline porous Si of the same thickness, obtained with the same electrochemical preparation. Excitation: 476 nm, 10 mW/cm^2. The inset shows the peak energy versus the porosity, estimated from the ratio of the integrated current to the measured thickness.

Further understanding of the basic recombination process in porous silicon is given by the following experiment: We perform *in situ* PL measurements with the sample in the electrochemical cell, but after disconnecting the current. With porous *c*-Si, photochemical

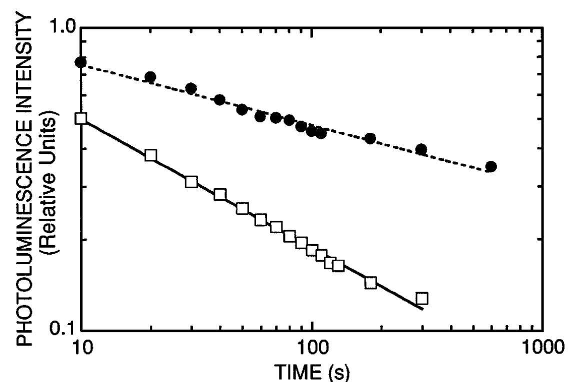

FIG. 4. Photodegradation of porous *a*-Si:H (circles) and porous *c*-Si (squares) under UV irradiation in air at room temperature (351 nm, 150 mW/cm^2). The PL intensity is taken at the peak energy.

etching slowly reduces the size of the nanostructures resulting in a gradual blueshift of the PL (from about 1.4 to 2.2 eV) which is clearly explained by progressive wave-function localization [12]. The same experiment on a 1.5 eV emitting porous *a*-Si:H sample shows no shift, in spite of actual etch, demonstrating a markedly different PL mechanism from that of its crystalline counterpart. Amorphous silicon is a highly disordered material having an elastic scattering length smaller than 10 Å for thermalized carriers, and it is not surprising that no quantum confinement effect is found [13]. The high PL intensity could be interpreted in terms of the capture radius for nonradiative recombination, known to explain recombination in *a*-Si:H [14]. If the diameter of the nanostructures is less than the capture radius and if there is no surface recombination, the quantum efficiency is expected to increase markedly [15]. This requires a remarkably efficient surface passivation for the porous *a*-Si:H structures as found in *c*-Si [16]. The same model predicts a shift of the PL line towards higher energy upon decreasing of the size of the nanostructures (spatial confinement prevents electron-hole pairs from finding a state for radiative recombination with an energy as low as in the bulk material) [15]: We do obtain a small shift of the peak energy from 1.3 to 1.5 eV by changing the porosity (Fig. 3). The intensity and peak energy of the PL spectra of porous *a*-Si:H remain stable during several months of exposure to air. In contrast, porous *c*-Si oxidizes rapidly in air giving rise to a blueshift in the spectra (1.5 to 2 eV). Bulk *a*-Si:H contains some 10% of hydrogen whereas for *c*-Si the hydrogen is mostly confined to the surface, which might explain the difference of evolution in time.

In conclusion, as with *c*-Si, the porous material produced from *a*-Si:H shows a strong luminescence, the starting material—boron-doped *a*-Si:H—having no detectable luminescence. A striking difference between the electrochemistry of *a*-Si:H and that of *c*-Si is the appearance of an instability which limits the maximum thickness of porous material that can be produced to a fraction of a micrometer. We explain this instability by the large value of the resistivity of *a*-Si:H compared to that of the electrolyte. Also, taking advantage of the thin-film geometry of *a*-Si:H, we have been able to produce the porous material from undoped *a*-Si:H by electrical injection of holes rather than by the usual photoinjection of carriers. Our results point to a difference between the PL mechanism of porous *a*-Si:H and *c*-Si. We attribute the PL to spatial confinement of the photocreated carriers, which reduces the nonradiative recombination in the absence of surface recombination. This explains both the strong enhancement of PL and its shift from 1.3 to 1.5 eV when the porosity increases [15]. Because of the limited amount of porous silicon produced, the total luminescence is much weaker than what can be obtained with a very thick layer of porous material from crystalline silicon. Nevertheless, the density of PL (luminescence for the same thickness of porous material) is quite comparable. From a practical point of view, we believe that the possibility to produce inexpensive luminescent layers on large surfaces can be interesting for industrial applications.

We gratefully acknowledge the help of L. R. Tessler during the early part of this work and useful discussions with E. Bustarret.

[1] L. T. Canham, Phys. Status Solidi B **190**, 9 (1995).
[2] K. H. Jung *et al.,* Appl. Phys. Lett. **61**, 2467 (1992).
[3] E. Bustarret, M. Ligeon, and L. Ortega, Solid State Commun. **83**, 461 (1992).
[4] E. Bustarret *et al.,* Mater. Res. Soc. Symp. Proc. **283**, 39 (1993).
[5] E. Bustarret, M. Ligeon, and M. Rosenbauer, Phys. Status Solidi B **190**, 111 (1995).
[6] R.L. Smith and S.D. Collins, J. Appl. Phys. **71**, R1 (1992).
[7] R.A. Street, *Hydrogenated Amorphous Silicon*, Cambridge Solid State Science Series (Univ. Press, Cambridge, Cambridge, 1991).
[8] R.B. Wehrspohn, J.-N. Chazalviel, F. Ozanam, and I. Solomon (to be published).
[9] M.A. Lampert and P. Mark, *Carrier Injection in Solids* (Academic, New York, 1970).
[10] I. Solomon, R. Benferhat, and H. Tran-Quoc, Phys. Rev. B **30**, 3422 (1984).
[11] T. Unagami and K. Kato, Jpn. J. Appl. Phys. **16**, 165 (1977).
[12] F. Ozanam, J.-N. Chazalviel, and R. B. Wehrspohn (to be published).
[13] This result stands in contrast with the quantum confinement effects in multilayers of amorphous films reported by D. J. Lockwood *et al.,* Phys. Rev. Lett. **76**, 539 (1996); however, comparison is difficult due to the different nature and structure of the materials.
[14] R. A. Street, Adv. Phys. **30**, 593 (1980).
[15] M. J. Estes and G. Moddel, Appl. Phys. Lett. **68**, 1814 (1996).
[16] J. M. Rehm *et al.,* Appl. Phys. Lett. **66**, 3669 (1995).